

1 **Title:** A compendium of predicted growths and derived symbiotic relationships between 803
2 gut microbes in 13 different diets

3

4 Rohan Singh, Anirban Dutta, Tungadri Bose*, Sharmila S. Mande*

5

6 TCS Research, Tata Consultancy Services Ltd., 54-B Hadapsar Industrial Estate, Pune, 411

7 013, India

8

9 *Corresponding authors

10

11 **Email Correspondence**

12 Tungadri Bose tungadri.bose@tcs.com

13 Sharmila S Mande sharmila.mande@tcs.com

14

15 **Abstract**

16 Gut health is intimately linked to dietary habits and the microbial community (microbiota)
17 that flourishes within. The delicate dependency of the latter on nutritional availability is also
18 strongly influenced by symbiotic relationships (such as, parasitic or mutualistic) between the
19 resident microbes, often affecting their growth rate and ability to produce key metabolites.
20 Since, cultivating the entire repertoire of gut microbes is an infeasible task, metabolic models
21 (genome-based metabolic reconstructions) could be employed to predict their growth patterns
22 and interactions. Here, we have used 803 gut microbial metabolic models from the Virtual
23 Metabolic Human repository, and subsequently optimized and simulated them to grow on 13
24 dietary compositions. The presented pairwise interaction data (<https://osf.io/ay8bq/>) and the
25 associated bacterial growth rates are expected to be useful for (a) deducing microbial
26 association patterns, (b) diet-based inference of personalised gut profiles, and (c) as a
27 steppingstone for studying multi-species metabolic interactions.

28

29 **Keywords**

30 Gut microbiome, Symbiotic relationships, Dietary compositions; Metabolic simulations;
31 Metabolic interactions

32 INTRODUCTION

33 Metabolism in the host is complemented by the microbial community (microbiota) harboured
34 in its gut. The microbiota collectively possesses a larger repertoire of enzymes which helps in
35 digestion and nutrient uptake from sources such as, complex carbohydrates [1]. Microbes also
36 synthesize and make available different key nutrients such as, essential amino acids, vitamins
37 and short chain fatty acids [2,3]. Consequently, imbalances (i.e., dysbiosis) in the gut
38 microbiota impacts an individual's health and has been linked to many diseases like
39 inflammatory bowel disease, obesity, type II diabetes, etc. [4–8]. Microbiome usually evolves
40 as a complex community [9] and it is imperative to investigate metabolic interconnection and
41 resultant interactions among them. While many microbiome studies derive inferences based
42 on the correlation of abundances (or cooccurrences) of gut microbial species, often so in a
43 disease or a dietary context [10,11], they seldom focus on their 'metabolic communication'.
44 Deducing such metabolic communications are often cumbersome, time consuming and costly;
45 given that majority of gut micro-organisms are not cultivable under *in-vitro* conditions [12].

46

47 Rapid advancement in genome sequencing in recent years have provided new impetus for
48 development of high-quality genome-scale metabolic models which can aid in microbial
49 metabolic network analysis. In addition to the genomic information, these metabolic models
50 can also be adapted to use multi-omics data (viz., proteomics, transcriptomics, metabolomics,
51 etc.) to replicate the metabolic behaviour of an organism under specific environmental
52 conditions, such as nutrient availability, stresses, co-culturing, etc. [13,14]. Earlier works by
53 independent research groups have established that pairwise interactions are the major drivers
54 of bacterial communities, as opposed to their higher-order interactions [9,15]. Metabolic
55 exchanges between two species could exemplify the nature of interactions that occurs

56 between them [16,17]. This is especially pivotal while considering environmental factors,
57 such as diet which could strongly drive the microbial composition and intrinsic metabolic
58 behaviour inside the gut [18]. Therefore, a joint genome-scale reconstruction of two different
59 organisms, in conjunction with Flux Balance Analysis (FBA) [1,8,16,19–21], could elicit
60 metabolic patterns that would define their innate relationship within a dietary/ nutrient
61 regimen (Dai et al., 2019; Heinken et al., 2019; Perisin & Sund, 2018). This has been
62 famously exemplified by Klitgord and Segrè [23], wherein the authors examined paired
63 combinations of seven metabolically reconstructed microbes (models) to identify nutrient
64 environments that induced symbiotic relations, which would otherwise deter growth in
65 isolated condition. This involved a combinatorial approach in determining media that led to
66 emergent mutualistic dependence through bidirectional exchange of nutrients necessary for
67 growth. It was also surmised that environmental/ nutrient fluctuations could have more
68 profound effect on microbial symbiosis than their genetic (or reactionary) perturbations.
69 Along the same lines, it has been shown that cooperative behaviour occurs when paired-
70 microbes have fewer common growth promoting metabolites [24]. Another study on
71 microbial consortia showed that these pairs/ consortia could produce new metabolites which
72 were otherwise absent in mono-cultures [25]. Some earlier metabolic modelling efforts in this
73 direction have also highlighted the capacity of paired models to produce metabolites which
74 were non-existent in their secluded form, as well as presented examples of the paired models’
75 increased potential of producing metabolites as compared to the additive sum of the
76 metabolite fluxes in their ‘mono-culture’ simulations [21].

77

78 These studies demonstrate the importance of studying interspecies relationships delineating
79 their mutualistic or inhibitory tendencies with each other in a case dependent manner. Our

80 work finds its basis in the above premise, explores the same in context of a human gut habitat,
81 and provides an extensive collection of potential interactions for all gut microbes for which
82 viable metabolic models were available from the VMH (Virtual Metabolic Human) repository
83 (Noronha et al., 2019). The potential interactions are derived from pairwise FBA simulations
84 of gut microbes mimicking their growth in 13 different dietary conditions. Having access to a
85 dietary “interactome”, could provide contextual guidance and justification towards elucidating
86 underlying relations amongst gut microbes, especially so while drawing inference from such
87 relationships determined through microbial abundance-based correlations. Furthermore, one
88 can also posit an approach for delineating key microbial growth deviations within or inter
89 dietary compositions, that would be helpful in understanding individual gut microbiome
90 profiles during a comparative analysis. The pairwise interaction type (as well as growth
91 potential) data for different diet types presented in this work essentially represents a semi-
92 exhaustive collection of gut bacterial ‘dyads’ (the smallest unit of interaction in a social
93 network/ group) and lays the foundation for progressively building onto as well as studying
94 larger gut bacterial networks/ ecosystems.

95

96

97 **RESULTS**

98 Metabolic simulations, based on flux balancing principles, were performed to gauge the
99 growth potential of gut microbes under varying diet conditions. A total of 818 metabolic
100 models resembling human gut associated microbes and 13 diet constraints imitating nutrient
101 availability (to gut microbes) in different dietary habits were used (see MATERIALS AND
102 METHODS). Simulations were performed for single organism models as well as paired
103 organism models to mimic growth of gut microbes in both mono-culture and co-culture

104 conditions under different diet conditions. Further, for each of the diet types, interactions
105 between a pair of microbes was determined from the change in growth rates of the two
106 organisms under co-culture (paired) and mono-culture conditions (see MATERIALS AND
107 METHODS).

108

109 **Technical validation against earlier AGORA simulations**

110 The obtained growth rates of the metabolic models representing the gut microbial species,
111 both in mono-culture and co-culture simulations, were benchmarked against the results
112 presented by Magnusdottir et al. [16], who had employed AGORA models (v1.0) in their
113 study. Since their simulation outcomes were reported for only two diet conditions, viz., High-
114 Fiber (AGORA) and Western (AGORA) diet, the evaluation could be performed for these two
115 diets only. For the 768 microbial species (metabolic models) which were common between
116 AGORA (version v1.0) [16] and our present work, we found strong correlation in their single
117 model (mono-culture) growth rates in both High-Fiber (AGORA) as well as Western
118 (AGORA) diets. SRC of 0.921 and 0.954 and PCC of 0.926 and 0.952 were observed for the
119 microbial growth rates in High-Fiber (AGORA) and Western (AGORA) diets respectively.
120 Similarly, comparison of the collective growth rates of the pairwise model (co-culture) also
121 showed good correlations for both the diets (considering 283,881 combinatorial pairs
122 common to both studies). In the co-cultured simulations, SRC of 0.903 and 0.933 and PCC of
123 0.85 and 0.87 were noted for High-Fiber (AGORA) and Western (AGORA) diets
124 respectively.

125

126 **Assessment of computed interactions in the context of literature evidences**

127 *Bifidobacterium* growth patterns in High Protein and High Fat diets: Using single model
128 simulation results in different VMH Diets, the mean growth rate of 39 different available
129 models of *Bifidobacterium* species was correlated to the main dietary constituents, namely
130 lipids (%), carbohydrates (%), protein (%), dietary fibers (mg), cholesterol (mg) and sugar
131 (mg) (as downloaded from nutrition information table provided in www.vmh.life/#nutrition).
132 Dietary fiber was found to have the strongest positive correlative emergent (PCC of 0.53) of
133 growth rate in single (mono-culture) model condition, and conversely, lipid of the diet
134 showed negative correlation (PCC of -0.49) to growth rate of *Bifidobacterium*. PCCs obtained
135 for the other factors, viz., carbohydrates, protein, cholesterol, and sugar (sucrose) were 0.22,
136 0.15, -0.19 and 0.24 respectively.

137

138 *Complementarity between Bacteroides thetaiotaomicron and Methanobrevibacter smithii:*
139 Two gut inhabiting organisms, *Methanobrevibacter smithii* and *Bacteroides thetaiotaomicron*,
140 are known to exhibit mutualistic (syntrophic) behaviour when grown in a polysaccharide
141 (dietary fiber) based diets [28,29]. We investigated if their syntrophic behavior (in fiber rich
142 diets), could also be replicated in our *in-silico* results. *M. Smithii* (model name
143 Methanobrevibacter_smithii_ATCC_35061) was found to have higher growth rate when co-
144 cultured (paired) with *B. thetaiotaomicron* (model name
145 Bacteroides_thetaiotaomicron_VPI_5482) in fiber rich diets. Its growth rate was seen to
146 increase by 4.51 folds in High-Fiber (AGORA) diet and by 1.44 folds in High-Fiber (VMH)
147 diet. For diets with poor fiber content (like Unhealthy diet and High-Fat with Low-Carb diet),
148 a reverse relationship of amensalism was observed wherein a drop in the growth rate of *M.*
149 *smithii* by 0.99 folds was found on co-culturing with *B. thetaiotaomicron*.

150

151 *Complementarity between Bifidobacterium adolescentis* and *Eubacterium hallii*: In yet
152 another instance, our simulation results could mimic the commensalistic behaviour between
153 *Eubacterium hallii* (model name *Eubacterium_hallii_DSM_3353*), a prominent butyrate-
154 producing bacterium [30] and *Bifidobacterium adolescentis* (model name
155 *Eubacterium_hallii_DSM_3353*), in diets which are rich in starch. Notably, it has been
156 reported that *E. hallii* by itself is not able to sustain in a starch rich diet and require assistance
157 from *B. adolescentis* for its survival [4]. In data presented in Table 1 this pair exhibited
158 commensalism in seven out of 13 diets and all of these diets feature higher starch content.
159 Three of the remaining diets (viz., Unhealthy, High-Fiber and Vegan) also had higher starch
160 content, but did not lead to any appreciable increase in the growth of *E. Hallii* (i.e $\geq 10\%$ of
161 growth rate) and their overall interaction was thus interpreted as neutralism for those diets.
162 Diets with poor starch content yielded negative interactions for this pair.

163

164

165 **DISCUSSION**

166 Genome scale metabolic reconstruction is one of the prime examples of genomics aiding
167 metabolomic research. Continuous growth in this field has propelled the gaining of metabolic
168 insights into complex problems like estimating the growth capacity of a microbe in a
169 nutritional environment [7,23] or cross feeding in a microbial community [17,21]. Hence, a
170 collection of such genome scale metabolic reconstructed models (like VMH repository -
171 www.vmh.life) along with several pre-determined dietary compositions provides an
172 opportunity to compile and build a vast resource of individual and/or symbiotic growth
173 capacity of gut microbes, tailored to these available diets. This, otherwise, via conventional
174 experimental procedures would be cumbersome, time consuming and costly if not infeasible.

175 Here in our study we have computed growths and interactions for 4,182,618 combinations of
176 available microbial pairs, and attempted validation of simulated growth rates and derived
177 symbiotic relationships to existing literature.

178

179 The ideal validations for the single model (mono-culture) and pairwise model (co-culture)
180 simulation results would be to compare the *in-silico* results with the experimental growth
181 rates under different diet types. However, given a multitude of factors, including difficulties
182 to replicate the diets in culture media, and challenges in growing most gut microbes in the
183 laboratory, the availability of experimental data to benchmark *in-silico* findings are limited.
184 Consequently, the publication presenting the original AGORA models (v1.0) [16] evaluated
185 simulation results using growth rates of only a single pair of gut microbes under a specialized
186 nutrient environment. This being a seminal publication on the topic, the results presented
187 therein were considered as a benchmark while performing the technical validations for our
188 current study. In brief, the mono-culture and co-culture growth rates of the 773 gut microbial
189 models (from AGORA v1.0), simulated under the two AGORA diets, viz., High-Fiber
190 (AGORA) and Western (AGORA) were used for this comparison. Subsequently, we have
191 also evaluated some of our predicted growth rates and derived symbiotic relationships against
192 experimentally observed diet-linked microbial growths and interaction patterns available from
193 literature.

194

195 It may be noted that the current version of AGORA models (v1.03), that has been used for
196 simulations performed in the current study, have been updated and refined since the original
197 publication [16]. The changes include rectification of false positive predictions of nutrient
198 uptakes within the model, implementation of improved gap-filing protocols on a new refined

199 growth media [31], and introduction of new pathway reactions from several studies like
200 aromatic amino acid degradation [32], putrefaction pathways in the gut [33], bile-acid
201 biosynthesis [7]. Given these differences in the models used as well as certain differences in
202 the methodology when compared to Magnusdottir et al. [16], some deviations pertaining to
203 the computed growth values, and the interactions derived, could be anticipated. The
204 methodological differences included usage of some revised reaction constraints (see Diet
205 Construction sub-section of MATERIALS AND METHODS), usage of COBRApy library
206 (python) in place of COBRA toolbox (MATLAB), usage of glpk solver (publicly available)
207 instead of the proprietary CPLEX solver (IBM, Inc.), using an adapted version of Mminte (a
208 python package) for paired model reconstruction [34] (see Code Usage in Appendix 1), and
209 employment of auxiliary flux coupling constraints, implemented within python (see
210 MATERIALS AND METHODS section and Code Usage in Appendix 1). Despite the
211 technical and methodological differences, the two studies displayed similar results in terms of
212 growth rates for the individual and paired organisms (See RESULTS section).

213

214 Additional validations were subsequently performed to check if the interaction patterns (and
215 the simulated growth rates) among a pair of microbes, as reported in this work, could replicate
216 the biologically observed phenomenon under different diet conditions. The three case studies
217 (as shown in RESULTS section) highlight the potential use that can be extended in this
218 regard.

219

220 Numerous studies have focussed attention to *Bifidobacterium*, an eminent gut inhabiting
221 species, which is particularly known for its probiotic interplay within host and with gut
222 microbial species [35,36]. Studies suggest that *Bifidobacterium* species grows poorly in diet

223 compositions made with high protein [37], and with high-fat and low-carbohydrate [38]. Our
224 simulation data gives similar indications for this species as shown by moderately negative
225 correlation to lipid content (See RESULTS section). It may be mentioned in this context that
226 Hwang and his co-workers [37] also evaluated the growth patterns of *Sutterella*, another gut
227 bacterium, in addition to *Bifidobacterium* and reported contrasting growth trends.
228 Unfortunately, the two models of *Sutterella* which have so far been reconstructed, were a
229 subset of 27 gut bacterial models (out of 803 used in this study) exhibiting no appreciable
230 change in growth rates across diet types and often very poor growth in mono-cultures
231 (Supplementary Table 1 in Appendix 1). Therefore, growth patterns of *Sutterella* in response
232 to different dietary constituents could not be assessed in course of technical validation for this
233 work. While the diet-invariant very low growth rates, possibly due to the inability of these
234 organisms to survive in isolation in the human gut, may be construed as a limitation of this
235 work, it may be noted that the growth rates of these organisms (including *Sutterella*) showed
236 significant variations in the co-culture simulations across different diet types.

237

238 Literature evidences also substantiates the simulation results i.e. growth rate derived
239 interaction paradigms, obtained in our study. For instance, *Bacteroides thetaiotaomicron*, one
240 of the most common gut species, and *Methanobrevibacter smithii*, a pre-dominant gut
241 microbe of *Archaea* domain, have been notably shown to have syntrophic relationship,
242 wherein *B. thetaiotaomicron* assists *M. smithii* to grow in polysaccharide (dietary fiber) based
243 diets [28,29]. Aligned with the experimental evidences, we observed commensalism in our
244 paired-model simulations between these two species in diets with high fiber content. On a
245 similar note, our derived interactions between gut microbes could also be validated for
246 another prominent experimental observation [4], which included *Bifidobacterium adolescentis*

247 and *Eubacterium hallii*. From the data presented in Table 1, the above interaction
248 phenomenon could be observed in diets which had higher starch contents, wherein the co-
249 cultured pair tend to display commensalism in favour of *E. hallii*.

250

251 Given the above, we believe that the provided resource would be useful in drawing inferences
252 from putative interactions between different gut organisms or from their overall growth
253 patterns across diverse set of pre-determined nutritional compositions. Our simulation data
254 could aid in providing clues (from metabolic perspective) to microbial interrelationships
255 derived solely from abundance-based correlations. And with a wider choice of dietary
256 compositions available to the users, there is an added propensity to mimic the diet of the
257 samples from which those correlations were derived, which makes the inferences/
258 justifications more meaningful.

259

260

261 **CONCLUSIONS**

262 The datasets generated in our study allows analysis/ data-inferences at intra/ inter diet level,
263 both of which enables investigation of diet induced growth patterns of an organism, a
264 taxonomic group or at the gross level for the entire microbiome samples. This could be useful
265 for investigation/ validation of any symbiotic relationships and growth deviations observed
266 for an organism of interest across single or several diets from experimental or *in-silico*
267 studies. Users can also utilize the pairwise growth values and deploy different growth cut-off
268 parameters for customizing definitions of symbiotic relationships and mining for such
269 interactions in a dataset of interest. In addition, users can make use of the organism's growth
270 rates/ interaction information for pruning microbial association networks derived from

271 abundance-based studies, as shown in an earlier study [17]. This data makes it possible to
272 filter or validate the edges of interaction networks of gut microbes from abundance-based
273 correlations and justify those connections from metabolic perspective. Furthermore, the
274 scripts provided in the repository allows for the extension of the framework to microbes
275 residing in any ecological niche and is thus expected to be beneficial for microbiologists,
276 ecological experts and other researchers working in allied areas.

277

278

279 **MATERIALS AND METHODS**

280 **Mono-culture (single model) simulation**

281 A total of 818 models representing the metabolic potential of human gut associated microbes
282 were retrieved from AGORA (assembly of gut organisms through reconstruction and
283 analysis) v1.03 (version dated 25-Feb-2019) hosted at www.vmh.life (Noronha et al., 2019)
284 (see Supplementary Table 2 in Appendix 1). While the current version of AGORA metabolic
285 models has been reported to be curated and refined based on experimental evidences in recent
286 scientific publications, for the purpose of the current study, each of the downloaded metabolic
287 models were further modified in the following manner:

288

289 (a) The reactions and metabolite identifiers within the models were converted to BiGG
290 identifier notation style so as to make it compatible and convenient for its use in with
291 COBRApy package [19].

292 (b) The lower bounds of the exchange reactions were modified to mimic the appropriate
293 diet constraints (see Diet Construction sub-section of MATERIALS AND

294 METHODS). If an exchange reaction of the model was absent in a diet's constraints
295 list, then the lower bound for that reaction was set to 0.

296

297 Finally, FBA was performed on each of the modified metabolic models under different diet
298 constraints (see Diet Construction sub-section of MATERIALS AND METHODS) using glpk
299 solver and COBRApy package in python [19]. The objective of the simulations was to predict
300 maximum possible growth of each of the bacteria (represented by their metabolic models),
301 when grown as anaerobic mono-culture under different diet conditions.

302

303 **Co-culture (paired model) simulation**

304 In order to replicate metabolic interactions among a pair of gut microbes, pairwise simulations
305 were carried out for 13 different diets (Table 2). Notably, the metabolic models representing
306 15 gut microbes showed infeasible FBA solution for growth optimization in at least one of the
307 diets under mono-culture condition and were excluded from the pairwise simulation
308 experiments. All combinations of the remaining 803 models were considered which totalled
309 to 322,003 pairs. The Mminte package [34] in python was employed to reconstruct the paired
310 models (representing a pair of gut microbes) using earlier suggested strategies (Magnúsdóttir
311 et al., 2017; Mendes-Soares et al., 2016). In brief, the models were joined into a common
312 lumen compartment which acted as an extracellular interface for the exchange of metabolites.
313 Additionally, to avoid scenarios where an organism (metabolic model) benefits the other
314 without producing any biomass (i.e. the objective function), flux coupling constraints were
315 introduced which stoichiometrically coupled every reaction to the biomass objective function,
316 as per the strategy suggested in earlier literature [7,16]. After introducing dietary constraints
317 to the extracellular compartment of the model (as followed for single model simulations),

318 FBA was run to simultaneously maximise growth of both organisms. Out of all the 322,003
319 model pairs, 331 model pairs could not be solved for either one or more VMH diets using
320 glpk solver that was used in this study. The output of each solvable pair, i.e. growth of each
321 organism in paired condition, single condition, percentage growth change between the
322 conditions and finally the interaction type was computed and saved for each diet. Thus, output
323 from 321,692 pairs for each VMH diet and 322,003 pairs for each AGORA diet were
324 tabulated and uploaded to the OSF Home repository.

325

326 **Determination of interaction**

327 Interaction types, between each pair of organisms, were evaluated from the simulated growth
328 rates of the organisms under co-culture (paired) and mono-culture conditions (Fig. 1). In line
329 with previous studies [16,21,34], whenever the growth rate of an organism changed by $\geq 10\%$
330 during co-culture ($[G_{org}]^P$), when compared to its growth rate in isolation ($[G_{org}]^I$), a
331 discernible interaction amounting to a symbiotic relationship was considered (Table 3).
332 Positive influence (+) was denoted for increased growth rate, negative influence (-) for a
333 decrease in growth rate, and no effect (0) if the growth rate did not change by at least 10%.
334 For every given pair of organisms (in a given diet type), one of the six different interactions
335 were assigned based on possible pairwise growth profile outcomes depicted in Table 3.

336

337 **Diet construction**

338 Human societies around the world have different diet preferences which differ widely in
339 nutrient composition. Gut microbes are known to exhibit alternate metabolic behaviour, and
340 consequently varying growth rates, in response to different diet types [4,18,39]. To mimic
341 this, the metabolic models of the gut microbes were simulated to grow on 13 different diet

342 types (Table 2), as mono- and bi-cultures (paired). Of the total 13 diets used in this study,
343 metabolic exchange constraints representing two diets (High-Fiber and Western) were
344 obtained from Magnúsdóttir et al. [16]. These two diets were then edited to incorporate
345 modified flux constraints for certain exchange reactions (such as setting lower bounds of
346 exchanges of acetaldehyde, 2-oxoglutarate, L-lactate, L-malate, succinate to 0
347 mmol/gDW/hr), as mentioned in AGORA v1.01 update (from www.vmh.life). The remaining
348 11 diets were retrieved from “Nutrition” section of VMH (from www.vmh.life). Since these
349 set of constraints defining the diet types by itself could not support growth for majority of
350 AGORA models, an adaptation protocol was additionally followed (as described in Heinken
351 et al., 2019). This protocol was adapted from “adaptVMHDietToAGORA” functionality of
352 Microbiome Modeling Toolbox [40] and was implemented in python for our study (see Code
353 Usage in Appendix 1).

354

355 **Data availability**

356 All data pertaining to this work has been tabulated and archived in OSF Home Data
357 Repository [41]. Details of the data records along with the format for each of the data files are
358 provided in Appendix 1 (see Data Record Information and Supplementary Tables 3, 4).

359

360 **AUTHOR CONTRIBUTIONS**

361 R.S., A.D., T.B. and S.S.M. conceived the idea, designed the protocol for data simulation and
362 analysis. R.S. implemented the codes, performed the simulation experiments and created the
363 data repository. R.S., A.D. and T.B. analysed the results. All authors contributed towards
364 drafting the final manuscript.

365

366

367 **CONFLICT OF INTEREST STATEMENT**

368 All authors are employed by the Research & Development division of Tata Consultancy
369 Services Ltd., a commercial company. However, the authors declare no competing financial
370 interests.

371

372

373 **DATA AVAILABILITY STATEMENT**

374 The simulation results obtained in this study has been deposited to ‘OSF Home’ repository
375 [41]. The data deposited to ‘OSF Home’ further comprise of the mono-culture and co-culture
376 simulation growth rates of 803 gut microbial species in 13 different diet types and the derived
377 symbiotic relationships between the gut microbial species. Description of the file formats for
378 these data records have been provided in Supplementary Tables 3 and 4 (Appendix 1). In
379 addition, a stand-alone program used for obtaining the co-culture simulation results is also
380 provided. This program accepts, as argument, a pair of genome scale metabolic model files
381 (in json or xml format) and a diet file (in json format) to generates co-culture growth rates of
382 the two microbes as well as infer the type of interaction among them. All these resources are
383 freely accessible for academic use.

384

385

386 **ABBREVIATIONS USED:**

387 FBA: Flux Balance Analysis

388 VMH: Virtual Metabolic Human

389 AGORA: Assembly of Gut Organisms through Reconstruction and Analysis

390 SRC: Spearman’s Rank Correlation Test scores

391 PCC: Pearson Correlation Coefficients

392

393 **REFERENCES**

- 394 [1] P. Sen, M. Orešič, Metabolic Modeling of Human Gut Microbiota on a Genome Scale:
395 An Overview, *Metabolites*. 9 (2019). <https://doi.org/10.3390/metabo9020022>.
- 396 [2] S.H. Duncan, K.P. Scott, A.G. Ramsay, H.J.M. Harmsen, G.W. Welling, C.S. Stewart,
397 H.J. Flint, Effects of Alternative Dietary Substrates on Competition between Human
398 Colonic Bacteria in an Anaerobic Fermentor System, *Appl Environ Microbiol.* 69 (2003)
399 1136–1142. <https://doi.org/10.1128/AEM.69.2.1136-1142.2003>.
- 400 [3] A. Shafquat, R. Joice, S.L. Simmons, C. Huttenhower, Functional and phylogenetic
401 assembly of microbial communities in the human microbiome, *Trends Microbiol.* 22
402 (2014) 261–266. <https://doi.org/10.1016/j.tim.2014.01.011>.
- 403 [4] A. Belenguer, S.H. Duncan, A.G. Calder, G. Holtrop, P. Louis, G.E. Lobley, H.J. Flint,
404 Two routes of metabolic cross-feeding between *Bifidobacterium adolescentis* and
405 butyrate-producing anaerobes from the human gut, *Appl. Environ. Microbiol.* 72 (2006)
406 3593–3599. <https://doi.org/10.1128/AEM.72.5.3593-3599.2006>.
- 407 [5] J.C. Clemente, L.K. Ursell, L.W. Parfrey, R. Knight, The Impact of the Gut Microbiota
408 on Human Health: An Integrative View, *Cell.* 148 (2012) 1258–1270.
409 <https://doi.org/10.1016/j.cell.2012.01.035>.
- 410 [6] H.S.P. de Souza, C. Fiocchi, D. Iliopoulos, The IBD interactome: an integrated view of
411 aetiology, pathogenesis and therapy, *Nature Reviews Gastroenterology & Hepatology.*
412 14 (2017) 739–749. <https://doi.org/10.1038/nrgastro.2017.110>.
- 413 [7] A. Heinken, D.A. Ravcheev, F. Baldini, L. Heirendt, R.M.T. Fleming, I. Thiele,
414 Systematic assessment of secondary bile acid metabolism in gut microbes reveals
415 distinct metabolic capabilities in inflammatory bowel disease, *Microbiome.* 7 (2019) 75.
416 <https://doi.org/10.1186/s40168-019-0689-3>.
- 417 [8] S. Magnúsdóttir, I. Thiele, Modeling metabolism of the human gut microbiome, *Curr.*
418 *Opin. Biotechnol.* 51 (2018) 90–96. <https://doi.org/10.1016/j.copbio.2017.12.005>.
- 419 [9] O.S. Venturelli, A.C. Carr, G. Fisher, R.H. Hsu, R. Lau, B.P. Bowen, S. Hromada, T.
420 Northen, A.P. Arkin, Deciphering microbial interactions in synthetic human gut
421 microbiome communities, *Mol Syst Biol.* 14 (2018).
422 <https://doi.org/10.15252/msb.20178157>.
- 423 [10] T. Kelder, J.H.M. Stroeve, S. Bijlsma, M. Radonjic, G. Roeselers, Correlation network
424 analysis reveals relationships between diet-induced changes in human gut microbiota
425 and metabolic health, *Nutr Diabetes.* 4 (2014) e122.
426 <https://doi.org/10.1038/nutd.2014.18>.
- 427 [11] L. Chen, V. Collij, M. Jaeger, I.C.L. van den Munckhof, A.V. Vila, A. Kurilshikov, R.
428 Gacesa, T. Sinha, M. Oosting, L.A.B. Joosten, J.H.W. Rutten, N.P. Riksen, R.J. Xavier,
429 F. Kuipers, C. Wijmenga, A. Zhernakova, M.G. Netea, R.K. Weersma, J. Fu, Gut
430 microbial co-abundance networks show specificity in inflammatory bowel disease and
431 obesity, *Nat Commun.* 11 (2020) 1–12. <https://doi.org/10.1038/s41467-020-17840-y>.
- 432 [12] O. Manor, R. Levy, E. Borenstein, Mapping the inner workings of the microbiome:
433 genomic- and metagenomic-based study of metabolism and metabolic interactions in the
434 human microbiome, *Cell Metab.* 20 (2014) 742–752.
435 <https://doi.org/10.1016/j.cmet.2014.07.021>.
- 436 [13] A. Rizvi, A. Shankar, A. Chatterjee, T.H. More, T. Bose, A. Dutta, K. Balakrishnan, L.
437 Madugulla, S. Rapole, S.S. Mande, S. Banerjee, S.C. Mande, Rewiring of Metabolic
438 Network in *Mycobacterium tuberculosis* During Adaptation to Different Stresses, *Front*
439 *Microbiol.* 10 (2019). <https://doi.org/10.3389/fmicb.2019.02417>.

- 440 [14] C.M.S. Kumar, K. Chugh, A. Dutta, V. Mahamkali, T. Bose, S.S. Mande, S.C. Mande,
441 P.A. Lund, Chaperonin Abundance Boosts Bacterial Fitness, *BioRxiv*. (2020)
442 2019.12.31.891820. <https://doi.org/10.1101/2019.12.31.891820>.
- 443 [15] R.M. Stubbendieck, C. Vargas-Bautista, P.D. Straight, Bacterial Communities:
444 Interactions to Scale, *Front Microbiol.* 7 (2016) 1234.
445 <https://doi.org/10.3389/fmicb.2016.01234>.
- 446 [16] S. Magnúsdóttir, A. Heinken, L. Kutt, D.A. Ravcheev, E. Bauer, A. Noronha, K.
447 Greenhalgh, C. Jäger, J. Baginska, P. Wilmes, R.M.T. Fleming, I. Thiele, Generation of
448 genome-scale metabolic reconstructions for 773 members of the human gut microbiota,
449 *Nat. Biotechnol.* 35 (2017) 81–89. <https://doi.org/10.1038/nbt.3703>.
- 450 [17] D. Dai, T. Wang, S. Wu, N.L. Gao, W.-H. Chen, Metabolic Dependencies Underlie
451 Interaction Patterns of Gut Microbiota During Enteropathogenesis, *Front. Microbiol.* 10
452 (2019). <https://doi.org/10.3389/fmicb.2019.01205>.
- 453 [18] C.D. Filippo, D. Cavalieri, M.D. Paola, M. Ramazzotti, J.B. Poullet, S. Massart, S.
454 Collini, G. Pieraccini, P. Lionetti, Impact of diet in shaping gut microbiota revealed by a
455 comparative study in children from Europe and rural Africa, *PNAS.* 107 (2010) 14691–
456 14696. <https://doi.org/10.1073/pnas.1005963107>.
- 457 [19] A. Ebrahim, J.A. Lerman, B.O. Palsson, D.R. Hyduke, COBRApy: COstraints-Based
458 Reconstruction and Analysis for Python, *BMC Systems Biology.* 7 (2013) 74.
459 <https://doi.org/10.1186/1752-0509-7-74>.
- 460 [20] J.D. Orth, I. Thiele, B.Ø. Palsson, What is flux balance analysis?, *Nat Biotechnol.* 28
461 (2010) 245–248. <https://doi.org/10.1038/nbt.1614>.
- 462 [21] M.A. Perisin, C.J. Sund, Human gut microbe co-cultures have greater potential than
463 monocultures for food waste remediation to commodity chemicals, *Scientific Reports.* 8
464 (2018) 15594. <https://doi.org/10.1038/s41598-018-33733-z>.
- 465 [22] Systematic assessment of secondary bile acid metabolism in gut microbes reveals
466 distinct metabolic capabilities in inflammatory bowel disease | *Microbiome* | Full Text,
467 (n.d.). [https://microbiomejournal.biomedcentral.com/articles/10.1186/s40168-019-0689-](https://microbiomejournal.biomedcentral.com/articles/10.1186/s40168-019-0689-3)
468 3 (accessed August 30, 2020).
- 469 [23] N. Klitgord, D. Segrè, Environments that Induce Synthetic Microbial Ecosystems, *PLOS*
470 *Computational Biology.* 6 (2010) e1001002.
471 <https://doi.org/10.1371/journal.pcbi.1001002>.
- 472 [24] S. Freilich, R. Zarecki, O. Eilam, E.S. Segal, C.S. Henry, M. Kupiec, U. Gophna, R.
473 Sharan, E. Ruppín, Competitive and cooperative metabolic interactions in bacterial
474 communities, *Nature Communications.* 2 (2011) 589.
475 <https://doi.org/10.1038/ncomms1597>.
- 476 [25] H.-C. Chiu, R. Levy, E. Borenstein, Emergent Biosynthetic Capacity in Simple
477 Microbial Communities, *PLOS Computational Biology.* 10 (2014) e1003695.
478 <https://doi.org/10.1371/journal.pcbi.1003695>.
- 479 [26] N. A, M. J, J. Y, G. E, S. N, P. G, D. Ad, K. M, M. D, H. Hs, H. A, H. L, M. S, R. Da, S.
480 S, G. P, F. L, G. B, P. M, P. A, R. M, R. A, R. M, W. L, Ž. A, J. E, K. M, K. I, Z. A, S.
481 R, F. Rmt, T. I, The Virtual Metabolic Human database: integrating human and gut
482 microbiome metabolism with nutrition and disease, *Nucleic Acids Research.* 47 (2019).
483 <https://doi.org/10.1093/nar/gky992>.
- 484 [27] A. Noronha, J. Modamio, Y. Jarosz, E. Guerard, N. Sompairac, G. Preciat, A.D.
485 Daníelsdóttir, M. Krecke, D. Merten, H.S. Haraldsdóttir, A. Heinken, L. Heirendt, S.
486 Magnúsdóttir, D.A. Ravcheev, S. Sahoo, P. Gawron, L. Friscioni, B. Garcia, M.
487 Prendergast, A. Puente, M. Rodrigues, A. Roy, M. Rouquaya, L. Wiltgen, A. Žagare, E.

- 488 John, M. Krueger, I. Kuperstein, A. Zinovyev, R. Schneider, R.M.T. Fleming, I. Thiele,
489 The Virtual Metabolic Human database: integrating human and gut microbiome
490 metabolism with nutrition and disease, *Nucleic Acids Res.* 47 (2019) D614–D624.
491 <https://doi.org/10.1093/nar/gky992>.
- 492 [28] B.S. Samuel, J.I. Gordon, A humanized gnotobiotic mouse model of host-archaeal-
493 bacterial mutualism, *Proc. Natl. Acad. Sci. U.S.A.* 103 (2006) 10011–10016.
494 <https://doi.org/10.1073/pnas.0602187103>.
- 495 [29] B.S. Samuel, E.E. Hansen, J.K. Manchester, P.M. Coutinho, B. Henrissat, R. Fulton, P.
496 Latreille, K. Kim, R.K. Wilson, J.I. Gordon, Genomic and metabolic adaptations of
497 *Methanobrevibacter smithii* to the human gut, *PNAS.* 104 (2007) 10643–10648.
498 <https://doi.org/10.1073/pnas.0704189104>.
- 499 [30] J. Tap, S. Mondot, F. Levenez, E. Pelletier, C. Caron, J.-P. Furet, E. Ugarte, R. Muñoz-
500 Tamayo, D.L.E. Paslier, R. Nalin, J. Dore, M. Leclerc, Towards the human intestinal
501 microbiota phylogenetic core, *Environ. Microbiol.* 11 (2009) 2574–2584.
502 <https://doi.org/10.1111/j.1462-2920.2009.01982.x>.
- 503 [31] M. Tramontano, S. Andrejev, M. Pruteanu, M. Klünemann, M. Kuhn, M. Galardini, P.
504 Jouhten, A. Zelezniak, G. Zeller, P. Bork, A. Typas, K.R. Patil, Nutritional preferences
505 of human gut bacteria reveal their metabolic idiosyncrasies, *Nature Microbiology.* 3
506 (2018) 514–522. <https://doi.org/10.1038/s41564-018-0123-9>.
- 507 [32] D. Dodd, M.H. Spitzer, W. Van Treuren, B.D. Merrill, A.J. Hryckowian, S.K.
508 Higginbottom, A. Le, T.M. Cowan, G.P. Nolan, M.A. Fischbach, J.L. Sonnenburg, A
509 gut bacterial pathway metabolizes aromatic amino acids into nine circulating
510 metabolites, *Nature.* 551 (2017) 648–652. <https://doi.org/10.1038/nature24661>.
- 511 [33] H. Kaur, C. Das, S.S. Mande, In Silico Analysis of Putrefaction Pathways in Bacteria
512 and Its Implication in Colorectal Cancer, *Front Microbiol.* 8 (2017).
513 <https://doi.org/10.3389/fmicb.2017.02166>.
- 514 [34] H. Mendes-Soares, M. Mundy, L.M. Soares, N. Chia, MMinte: an application for
515 predicting metabolic interactions among the microbial species in a community, *BMC*
516 *Bioinformatics.* 17 (2016) 1–10. <https://doi.org/10.1186/s12859-016-1230-3>.
- 517 [35] P. Ruas-Madiedo, M. Gueimonde, M. Fernández-García, C.G. de los Reyes-Gavilán, A.
518 Margolles, Mucin Degradation by Bifidobacterium Strains Isolated from the Human
519 Intestinal Microbiota, *Appl Environ Microbiol.* 74 (2008) 1936–1940.
520 <https://doi.org/10.1128/AEM.02509-07>.
- 521 [36] A. O’Callaghan, D. van Sinderen, Bifidobacteria and Their Role as Members of the
522 Human Gut Microbiota, *Front Microbiol.* 7 (2016) 925.
523 <https://doi.org/10.3389/fmicb.2016.00925>.
- 524 [37] N. Hwang, T. Eom, S.K. Gupta, S.-Y. Jeong, D.-Y. Jeong, Y.S. Kim, J.-H. Lee, M.J.
525 Sadowsky, T. Unno, Genes and Gut Bacteria Involved in Luminal Butyrate Reduction
526 Caused by Diet and Loperamide, *Genes (Basel).* 8 (2017).
527 <https://doi.org/10.3390/genes8120350>.
- 528 [38] P.D. Cani, A.M. Neyrinck, F. Fava, C. Knauf, R.G. Burcelin, K.M. Tuohy, G.R. Gibson,
529 N.M. Delzenne, Selective increases of bifidobacteria in gut microflora improve high-fat-
530 diet-induced diabetes in mice through a mechanism associated with endotoxaemia,
531 *Diabetologia.* 50 (2007) 2374–2383. <https://doi.org/10.1007/s00125-007-0791-0>.
- 532 [39] L.-G. Jang, G. Choi, S.-W. Kim, B.-Y. Kim, S. Lee, H. Park, The combination of sport
533 and sport-specific diet is associated with characteristics of gut microbiota: an
534 observational study, *J Int Soc Sports Nutr.* 16 (2019) 21. <https://doi.org/10.1186/s12970-019-0290-y>.
- 535

- 536 [40] F. Baldini, A. Heinken, L. Heirendt, S. Magnusdottir, R.M.T. Fleming, I. Thiele, The
537 Microbiome Modeling Toolbox: from microbial interactions to personalized microbial
538 communities, *Bioinformatics*. 35 (2019) 2332–2334.
539 <https://doi.org/10.1093/bioinformatics/bty941>.
540 [41] R. Singh, A. Dutta, T. Bose, S. Mande, Gut Microbe Simulation Data Resource, (2020).
541 <https://doi.org/None>.
542

543

TABLES

544 **Table 1:** Pairwise relationship between *Eubacterium hallii* and *Bifidobacterium adolescentis*
 545 under different dietary simulations.
 546

Interaction	% change in growth rate (<i>E. hallii</i>)	% change in growth rate (<i>B. adolescentis</i>)	Diet	Starch Uptake (mmol/gDW/hr)
Amensalism	-61.93	0.00	High-Fat Low-Carb	0.005
Neutralism	-1.59	0.00	Unhealthy	3.176
Neutralism	0.00	0.00	High-Fiber	3.572
Neutralism	8.27	0.00	Vegan	2.444
Commensalism	33.31	0.00	Vegetarian	3.273
Commensalism	47.32	0.00	EU Average	2.616
Commensalism	54.08	0.00	High-Protein	2.145
Commensalism	66.65	0.00	Type-2 Diabetes	2.010
Commensalism	83.11	0.00	Gluten Free	5.295
Commensalism	96.92	0.00	Mediterranean	3.248
Commensalism	168.93	0.00	DACH	2.969
Parasitism	314.82	-45.55	Western (Agora)	0.257
Parasitism	385.40	-58.07	High-Fiber (Agora)	0.068

547

548

549 **TABLE 2:** List of the diets used in this study along with the number of their reactionary
 550 constraints and the literature where they were first defined.
 551

Diet Type	Description	Source	Total Reactions
DACH	A recommended diet composition made by the society for Nutrition in Switzerland Germany and Austria, to guarantee healthy nutrition for an adult human being.		162
EU Average	A diet derived from a large nutrient based survey done where the participants are from many European nations different age groups		162
Gluten Free	A diet devoid of gluten for individuals with gluten intolerance		162
High-Fat Low-Carb	The high fat diet should imitate a ketogenic diet (as recommended for epileptic patients), which is composed of 1,7% of energy of carbohydrates, 70% of energy of lipids and 24% of energy of proteins.		162
High-Protein	A composition typically representing a sports-based diet for athletes.		162
High-Fiber	This diet composing of high amounts of fibers than a plant-based diet (i.e. vegan diet) and includes animal derived products in it	[25]	162
Mediterranean	This diet is consumption of fresh plant foods, dairy products, poultry, and fish, but minimizes on consumption of processed food, red meat, and olive oil (as fat source)		162
Type-2 Diabetes	A diet for type 2 diabetes patient is which constitutes high content of vitamins (eg. Vitamin C & E) and minerals, but is low in kcal		162
Vegan	A plant-based diet with no consumption of animal derived products		162
Vegetarian	An ovo-lacto-vegetarian diet which constitutes consumption of dairy, egg products, fruits and vegetables		162
Unhealthy	It contains very low amount of dietary fibers, but high kcal amount, simple sugars, saturated fatty acids, and cholesterol		162
High-Fiber (AGORA)	A diet with higher fiber content but lower in simple sugars and fat content	[16]	177
Western (AGORA)	A diet with high amounts of simple sugars and fat content and but low in fiber content		175

552
 553

554 **TABLE 3:** Pairwise interaction patterns based on the growth profile outcomes of the two
555 organisms constituting a (paired) co-culture simulation experiment.
556

Type of Paired Interaction	Description	Abbreviation
Amensalism	One organism deteriorates in growth while the other organism remains unaffected	(0, -) or (-, 0)
Commensalism	One organism increases in growth while the other organism remains unaffected	(0, +) or (+, 0)
Competition	Both organisms suffer from drop in their individual growths under paired condition	(-, -)
Mutualism	Both organisms have augmentation in their individual growths under paired condition	(+, +)
Neutralism	Growths of both organisms remain unchanged under paired condition	(0, 0)
Parasitism	Growth of one organism diminishes while the same increases in the other organism	(-, +) or (+, -)

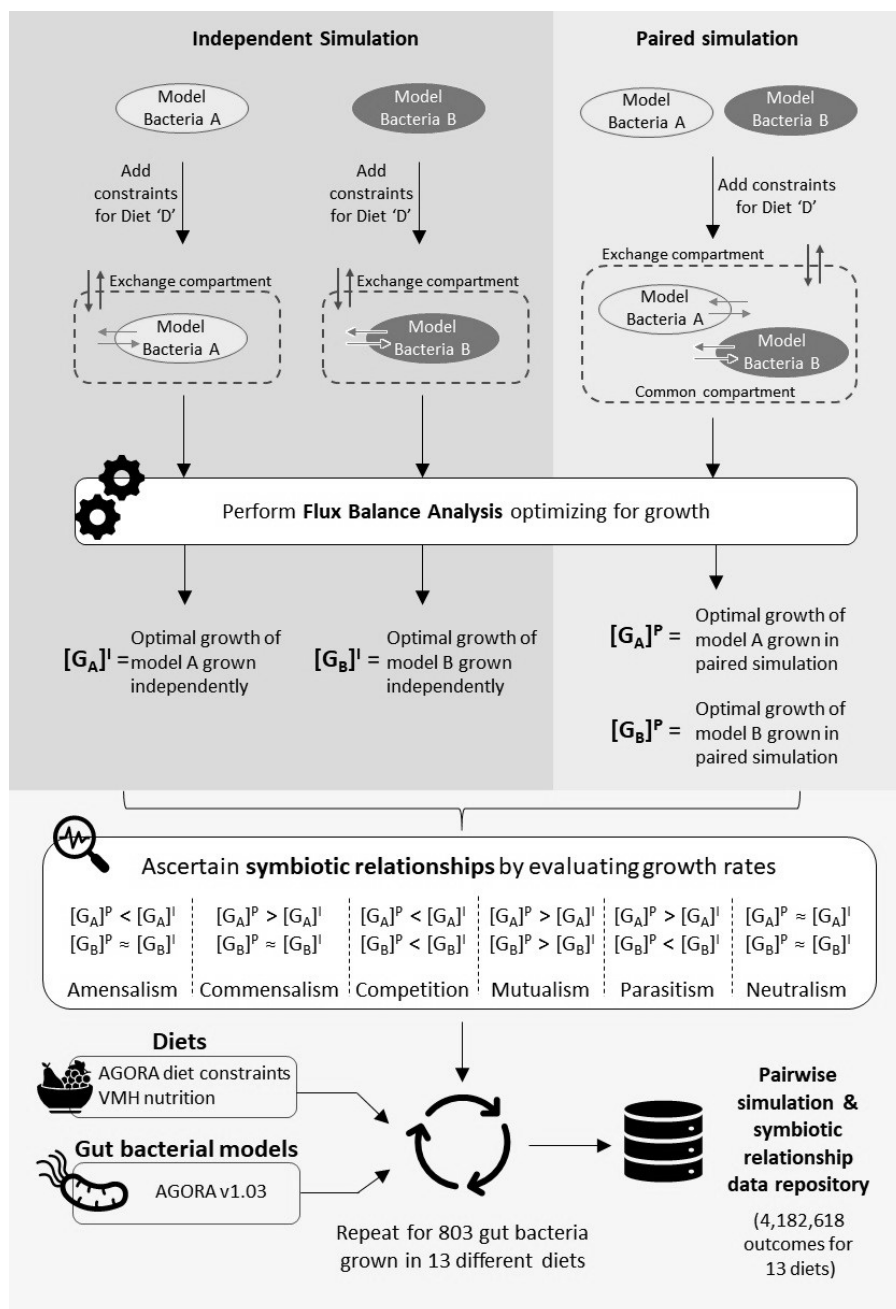
Abbreviation keys - 0: Unaffected; +: positive change; -: negative change

557
558

559

FIGURES

560

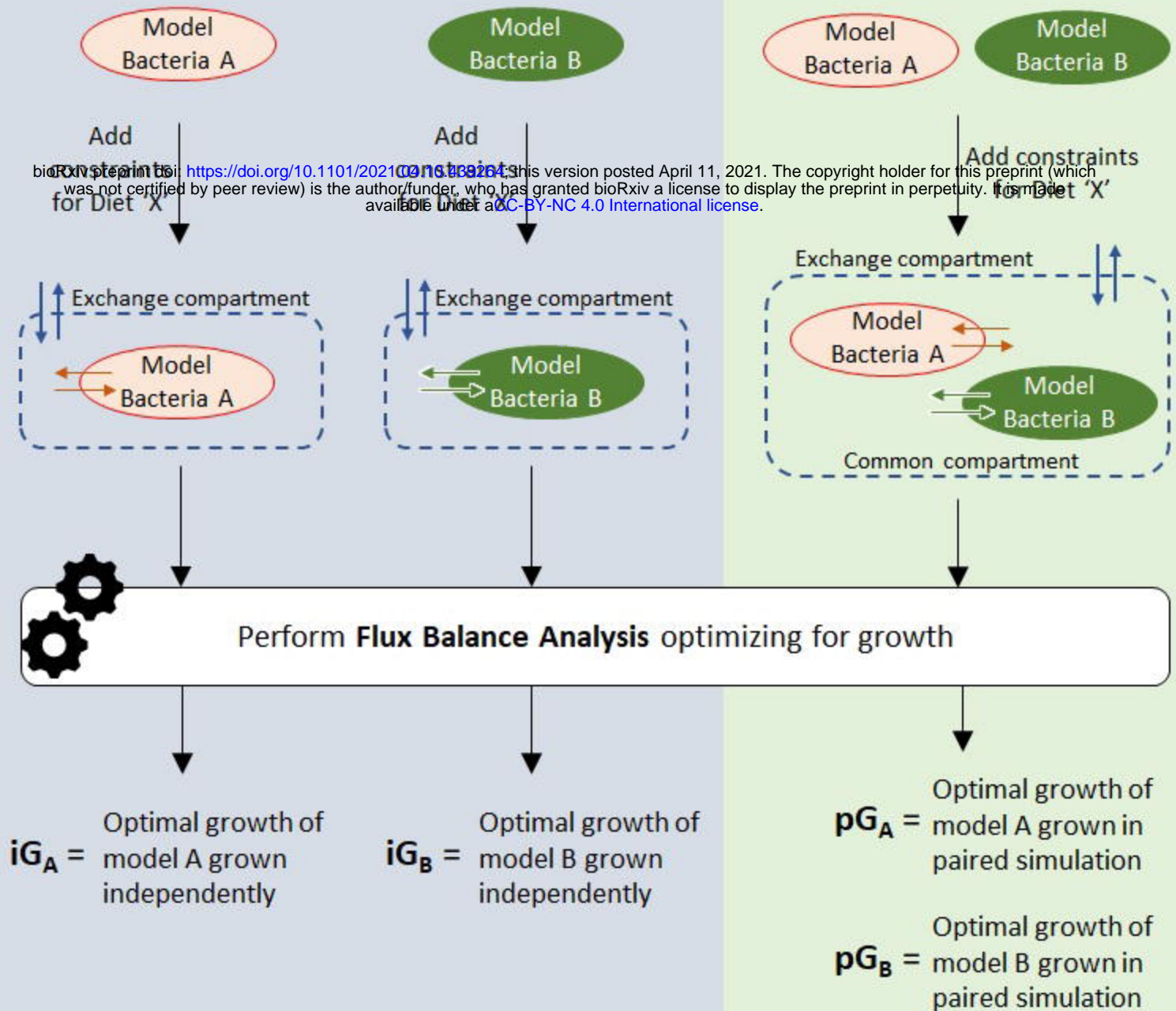


561

Figure 1: Schematic representation of the process followed for determining pairwise symbiotic interactions between gut microbial species. The '>' and '<' symbols denote that the growth of an organism in paired simulations $[G_{org}]^P$ (mimicking co-cultures) deviates at least by 10% or more when compared to its growth when simulated independently $[G_{org}]^I$ (mimicking monoculture).

Independent Simulation

Paired simulation



Ascertain **sybiotic relationships** by evaluating growth rates

$pG_A < iG_A$	$pG_A > iG_A$	$pG_A < iG_A$	$pG_A > iG_A$	$pG_A > iG_A$	$pG_A \approx iG_A$
$pG_B \approx iG_B$	$pG_B \approx iG_B$	$pG_B < iG_B$	$pG_B > iG_B$	$pG_B < iG_B$	$pG_B \approx iG_B$
Amensalism	Commensalism	Competition	Mutualism	Parasitism	Neutralism

Diets

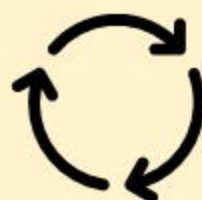


AGORA reconstruction
VMH nutrition



Gut bacterial models

AGORA v1.03
(www.vmh.life)



Repeat for 818 gut bacteria
grown in 13 different diets



**Pairwise
simulation &
sybiotic
relationship
data repository**

(4,182,618
outcomes for
13 diets)